Trajectory of Rotor Resistance for Detecting Broken Rotor Bars of Asynchronous Machines

Raya A. K. Aswad[1], Laszlo Szamel[2] and Bassim M. H. Jassim[3]

[1,2] Budapest University of Technology and Economics, Faculty of Electrical Engineering and Informatics, Department of Electric Power Engineering, Műegyetem rkp. 3, H-1111 Budapest, Hungary
raya.aswad@edu.bme.hu, szamel.laszlo@vet.bme.hu

[3] University of Baghdad, College of Engineering, Department of Electrical Engineering, 10071 Baghdad, Iraq; bassim.jassim@uob.edu.iq

Abstract: While each industrial sector aims to provide uninterrupted customer service, unplanned shutdowns are undoubtedly undesirable. For this purpose, many studies have been dedicated to fault detection in early stages, to make correct and timely decisions to avoid sudden shutdowns. This paper focuses on detecting broken rotor bar faults in asynchronous motors, industry's dominant machines. A model-based-parameter estimation approach is presented, to detect this fault under variable load conditions. The simulation results demonstrate deviations in the motor's parameters across different scenarios of broken rotor fault intensity and under varying loads. Moreover, the results imply a linear relationship between the fault's intensity and rotor resistance variations. Consequently, the approach is not only to detect the presence of the fault, but to also to provide information concerning the fault's severity.

Keywords: Asynchronous motors; Broken rotor fault; Model-based; Parameter estimation

1 Introduction

The ultimate goal for detection systems is to minimize shutdown time and maximize the efficiency of an operating system. As a matter of fact, asynchronous machines are widely employed in various industrial sectors, due to their impeccable characteristics. Hence, several studies are devoted to fault detection and diagnosis in these machines. A review study given in [1], covered related works within the timeframe from 1990 to 2022. Yet, this research area is still active, and developing an optimal diagnosis system receives substantial concern from the researchers. This paper aims to provide a detection system for a Broken Rotor Bar (BRB) in asynchronous machines. The following paragraphs will provide insight into the literature review of the most recent related works.

Literature review:

Broken rotor bar, bearing, eccentricity, and inter-turn faults detection using a neural network is considered in [2], the neural system was trained with current and voltage signals of a total of 5418 files with a signal duration of 20 seconds. The accuracy of the suggested system was 72%, and the insufficient information in the data justifies this number. The authors recommended further studies considering increasing the measurement frequency to make the effect of faults defects visible in high frequency spectrum of the input signals. Furthermore, they signified that increasing the signal duration could result in accurate fault classification with a drawback of computation-time increment.

One of the most widely used methods for faults identification is based on current signal analysis, which is also referred to as Motor Current Signature Analysis (MCSA). A comparison study between a traditional MCSA and similar methods like motor square current signature analysis, Park's vector square, Park-Hilbert, and Park's Vector Product Approach (PVPA) is shown in [3]. The study concluded that PVPA approach is highly sensitive to the presence of stator or rotor faults in asynchronous machines among the other approaches under load level variations. The advantage of such detection methods lies in analyzing current signals, which are easy to gather by non-invasive sensors. Using two current sensors and calculating the third, is more convenient for a balanced supply. Nevertheless, unbalanced supply operation and machine asymmetry harmonics can easily mislead these methods [1].

In [4], an approach based on advanced transient current signal analysis has emerged to identify malfunctioning machines with a broken rotor fault. The approach tracks the 'V' shaped pattern in the time-frequency plane of the signal.

A broken rotor bar influences the smoothness of the healthy stator currents and leads to the generation of an envelope. This envelope has been used for extracting fault's features and fed to a neural network system for detecting different classes of broken rotor bars at full load operation [5]. Promising results have been obtained with almost 100% accuracy; however, the main drawback of this strategy was highlighted as it is impossible to use this method if the healthy data of the asynchronous motor is unavailable. Furthermore, this paper did not examine this system at light load.

A possible way to detect the broken rotor bar fault without training by measuring healthy and faulty data is through model-based strategies. This has been addressed in [6] a model-based support vector classification was implemented to detect broken rotor bar faults at full load conditions. Nonetheless, the method cannot identify the severity of the presented fault. Moreover, the capability of detection under the model's parameters uncertainty, has not been proven.

The parameter estimation method is introduced as a superior diagnosis method when it comes to speed variation for a machine fed by an inverter. Unlike the signal spectral analysis methods, which rely on detecting the frequency spectrum that

varies with the speed variation [7] [8]. In [7], stator and broken rotor bar faults in three-phase induction machines are diagnosed by estimating the parameters of a faulty model where prior knowledge of the electrical parameters of the motor is required. Moreover, the speed signal was used for parameter estimation, rendering the suggested method as an intrusive diagnosis method.

This paper investigates the parameter estimation method to detect a broken rotor fault. Particularly, following the trajectory of rotor resistance to achieve this goal. Even though the variation of the rotor resistance of a malfunction machine with a broken rotor fault was exposed in [9]. In [10], the same approach was employed with respect to a machine fed via a drive with close-loop field-oriented control. Both studies used an extended Kalman filter for the parameter estimation. However, load level variation was not considered in these studies, and another offline detection method by FFT is suggested in [10] to mitigate the load variation effect on the rotor resistance. Here, variation of the rotor resistance at no load, half load, and full load is revealed in this article.

2 Modeling of Asynchronous Motor with Broken Rotor Bar

For the comprehension of an asynchronous motor behavior under a broken rotor fault, this section gives a mathematical representation of a faulty machine with a variable number of broken rotor bars. Moreover, model-based detection methods rely mainly on using a machine model. Yet, providing a simple model with sufficient details to describe the fault effects is very important [11].

The electrical and mechanical dynamic equations of a healthy asynchronous motor in the qd0 reference frame are as follows [12]:

$$\boldsymbol{v}_s^{qd0} = \boldsymbol{r}_s^{qd0}\boldsymbol{i}_s^{qd0} + \omega\begin{pmatrix} 0 & 1 & 0 \\ -1 & 0 & 0 \\ 0 & 0 & 0 \end{pmatrix}\boldsymbol{\lambda}_s^{qd0} + \frac{d\boldsymbol{\lambda}_s^{qd0}}{dt}, \omega = \frac{d\theta}{dt} \tag{1}$$

$$\boldsymbol{v}_r^{qd0} = \boldsymbol{r}_r^{qd0}\boldsymbol{i}_r^{qd0} + (\omega - \omega_r)\begin{pmatrix} 0 & 1 & 0 \\ -1 & 0 & 0 \\ 0 & 0 & 0 \end{pmatrix}\boldsymbol{\lambda}_r^{qd0} + \frac{d\boldsymbol{\lambda}_r^{qd0}}{dt} \tag{2}$$

$$\begin{bmatrix} \boldsymbol{\lambda}_s^{qd0} \\ \boldsymbol{\lambda}_r^{\prime qd0} \end{bmatrix} = \begin{bmatrix} L_{1s}+L_m & 0 & 0 & L_m & 0 & 0 \\ 0 & L_{1s}+L_m & 0 & 0 & L_m & 0 \\ 0 & 0 & L_{1s} & 0 & 0 & 0 \\ L_m & 0 & 0 & L'_{1r}+L_m & 0 & 0 \\ 0 & L_m & 0 & 0 & L'_{1r}+L_m & 0 \\ 0 & 0 & 0 & 0 & 0 & L'_{1r} \end{bmatrix} \begin{bmatrix} \boldsymbol{i}_s^{qd0} \\ \boldsymbol{i}_r^{\prime qd0} \end{bmatrix} \tag{3}$$

$$T_{em} = \frac{3p}{4}\left(\lambda_{ds}i_{qs} - \lambda_{qs}i_{ds}\right) \tag{4}$$

$$\omega_r = \frac{1}{J}\int\left(T_{em} - T_l - T_{damp}\right)dt \tag{5}$$

In the above equations, the subscripts s and r refer to the stator and rotor reference frames. The column vectors $\boldsymbol{v}_s^{qd0}$, $\boldsymbol{i}_s^{qd0}$, $\boldsymbol{\lambda}_s^{qd0}$, $\boldsymbol{v}_r^{qd0}$, $\boldsymbol{i}_r^{qd0}$, $\boldsymbol{\lambda}_r^{qd0}$ represent stator and rotor voltages, currents, and fluxes, respectively. Matrices $\boldsymbol{r}_s^{qd0}$ and $\boldsymbol{r}_r^{qd0}$ express the stator and rotor resistances. The variables θ, ω_r, L_{1s}, L'_{1r}, L_m, T_{em}, p, T_l, and T_{damp} represent the transformation angle from the ***abc*** reference frame to the ***qd0*** reference frame, the rotor speed, the stator leakage inductance, the rotor leakage inductance referred to the stator, the mutual magnetizing inductance, electromagnetic torque, the pole pairs, the load torque, and the damping torque, respectively.

A broken rotor bar can be mathematically represented by changing the values of rotor parameters. The faulty phase draws less current than the other unfaulty phases. Consequently, a nonlinear magnetic field will be generated between the stator and rotor due to the asymmetrical currents, which are also responsible for the induced harmonics in the stator currents [13]. The changes in the rotor inductances due to the broken rotor fault can be considered negligible compared to the rotor resistance changes. The changes in the rotor resistances in the abc reference frame can be described as follows [15]:

$$\boldsymbol{r}^{r*} = \begin{bmatrix} (r_r + \Delta r_{ra}) & 0 & 0 \\ 0 & (r_r + \Delta r_{rb}) & 0 \\ 0 & 0 & (r_r + \Delta r_{rc}) \end{bmatrix} \tag{6}$$

Where the variables Δr_{ra}, Δr_{rb}, and Δr_{rc} are the changes in the three-phase rotor resistances after the presence of the broken rotor fault. The value of per-phase rotor resistance r_r is given in equation (7):

$$r_r = \frac{(2N_s)^2}{N_b/3} r_b \tag{7}$$

where N_s, N_b, and r_b are symbols for the number of stator winding turns, the number of total rotor bars, and the rotor bar resistance, respectively.

The values of Δr_{ra}, Δr_{rb}, and Δr_{rc} can be obtained from the following equation:

$$\Delta r_{ra,b,c} = r^{r*} - r_r = \frac{(2N_s)^2}{(N_b/3) - n_{bb}} r_b - \frac{(2N_s)^2}{N_b/3} r_b = \frac{3n_{bb}}{N_b - 3n_{bb}} r_r \tag{8}$$

where n_{bb} is the number of broken rotor bars.

Transforming equation (6) into qd0 reference frame results in the following matrix:

$$\boldsymbol{r}_r{}^{*qd0} = \begin{bmatrix} r_{r11} & r_{r12} & r_{r13} \\ r_{r21} & r_{r22} & r_{r23} \\ r_{r31} & r_{r32} & r_{r33} \end{bmatrix} \tag{9}$$

Where,

$$r_{r11} = \frac{1}{3}(\Delta r_{ra} + \Delta r_{rb} + \Delta r_{rc}) + \frac{1}{6}(2\Delta r_{ra} - \Delta r_{rb} - \Delta r_{rc})\cos(2\theta_r) + \frac{\sqrt{3}}{6}(\Delta r_{rb} - \Delta r_{rc})\sin(2\theta_r)$$

$$\frac{\sqrt{3}}{6}(\Delta r_{rb} - \Delta r_{rc})$$

$$r_{r12} = \frac{-1}{6}(2\Delta r_{ra} - \Delta r_{rb} - \Delta r_{rc})\sin(2\theta_r) + \frac{\sqrt{3}}{6}(\Delta r_{rb} - \Delta r_{rc})\cos(2\theta_r)$$

$$r_{r13} = \frac{1}{3}(2\Delta r_{ra} - \Delta r_{rb} - \Delta r_{rc})\cos(\theta_r) - \frac{\sqrt{3}}{3}(\Delta r_{rb} - \Delta r_{rc})\sin(\theta_r)$$

$$r_{r21} = r_{r12}$$

$$r_{r22} = \frac{1}{3}(\Delta r_{ra} + \Delta r_{rb} + \Delta r_{rc}) - \frac{1}{6}(2\Delta r_{ra} - \Delta r_{rb} - \Delta r_{rc})\cos(2\theta_r) + \frac{\sqrt{3}}{6}(\Delta r_{rb} - \Delta r_{rc})\sin(2\theta_r)$$

$$r_{r23} = \frac{-1}{3}(2\Delta r_{ra} - \Delta r_{rb} - \Delta r_{rc})\sin(\theta_r) - \frac{\sqrt{3}}{3}(\Delta r_{ra} - \Delta r_{rc})\cos(\theta_r)$$

$$r_{r31} = \frac{1}{2}r_{r13}$$

$$r_{r32} = \frac{1}{2}r_{r23}$$

$$r_{r33} = \frac{1}{3}(\Delta r_{ra} + \Delta r_{rb} + \Delta r_{rc})$$

3 Broken Rotor Fault Detection Technique

A notable markup for the incidence of a broken rotor bar in an asynchronous motor is the machine's parameters changing. A model-based detection strategy is proposed in this article to delve into the variation of parameters and extract signs for the detection of this fault. The process chart of the method is given in Fig. 1.

The fault's features are supposed to be taken from the trajectory of rotor resistance; therefore, two nonlinear optimization methods are suggested for estimating the under-test machine's parameters. The Trust-Region Method (TRM) and Levenberg-Marquardt (LM) methods are used in this paper. Although other optimization methods employed in various applications [14-18] can also be utilized , one crucial reason for selecting TRM and LM methods is the need for a fast optimization process, which results in quicker BRB detection alarms.

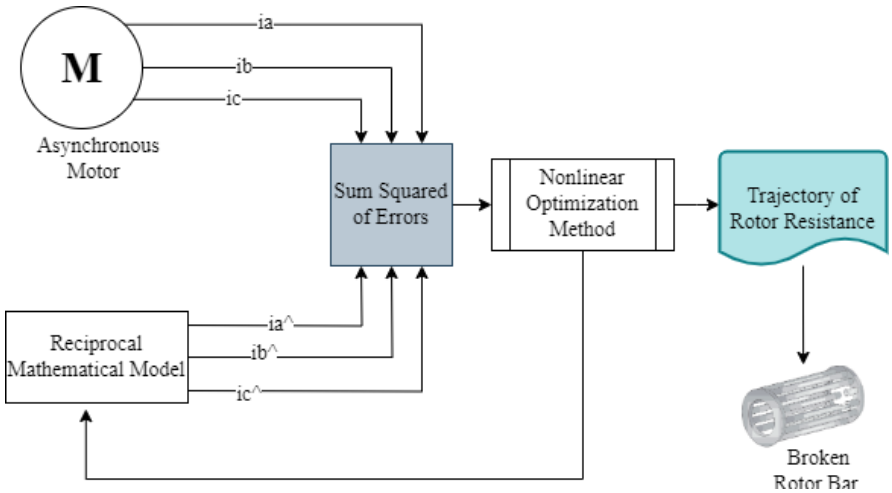

Figure 1
Process chart of broken rotor fault detection

The nonlinear optimization problem is as follows:

$$\left.\begin{aligned} Minimize\ f(\boldsymbol{X}) = \sum(ia - ia\hat{})^2 + (ib - ib\hat{})^2 + (ic - ic\hat{})^2 \\ \boldsymbol{X} = \{r_r, r_s, L_{1s}, L_{1r}, L_m, LL\} \end{aligned}\right\} \quad (10)$$

Where $f(\boldsymbol{X})$ is the cost function, which is the sum squared of errors between the three-phase stator currents of the machine under test and their reciprocal currents from the mathematical model. The solution for this problem is given in the vector $\boldsymbol{X}$, a new parameter is introduced in this vector that represents the percentage of load level (LL). Because it is necessary to take into consideration the effect of load on the parameters' behavior. The initial values of vector $\boldsymbol{X}$ parameters are fed into the mathematical model through a Matlab m-file, and then the model generates the corresponding stator currents, which are required in Eq. (10).

3.1 Trust-Region Method (TRM)

The TRM is regarded as the alternative optimization method to the classical line search methods, which might be trapped in the neighborhoods of saddle points [19]. To encapsulate the idea of the TRM, the process starts with an initial solution $\boldsymbol{X_0}$ and constructs a quadratic model using a Taylor series around the current solution, which simplifies the main cost function. Next, the quadratic function is minimized to obtain a minimal solution that represents a solution within a trust region. If the given solution is not the minimal, the method updates the size of the trust region and searches again for the optimal solution. The TRM process is as follows [20]:

1. Set initial a trust region boundary: radius $\Delta_0 > 0$: set $0 \leq \tau_1 < \tau_2 < 1$, $0 \leq \tau_3 < \tau_4$, upper radius limit $\Delta^- > 0$ and $0 \leq \epsilon \ll 1$

2. Calculate the gradient of the cost function as in Eq.(11).

$$g_k = \left[\frac{\partial f(x)}{\partial ia} \; \frac{\partial f(x)}{\partial ib} \; \frac{\partial f(x)}{\partial ic}\right] \tag{11}$$

3. Solve the quadratic problem to find the solution $\boldsymbol{d_k}$:

$$\left.\begin{aligned} \min q_k(\boldsymbol{d}) = {g_k}^T \boldsymbol{d} + \tfrac{1}{2}\, \boldsymbol{d}^T B_k \boldsymbol{d} \\ \text{Such that } \|\boldsymbol{d}\| \; < \Delta_k \end{aligned}\right\} \tag{12}$$

Where B_k is the approximate of the Hessian matrix given in Eq. (13), and $\|\boldsymbol{d}\|$ is the norm of the vector ***d.***

$$B_k = \begin{bmatrix} \frac{\partial^2 f(x)}{\partial^2 ia} & \frac{\partial^2 f(x)}{\partial^2 ia\, ib} & \frac{\partial^2 f(x)}{\partial^2 ia\, ic} \\ \frac{\partial^2 f(x)}{\partial^2 ib\, ia} & \frac{\partial^2 f(x)}{\partial^2 ib} & \frac{\partial^2 f(x)}{\partial^2 ib\, ic} \\ \frac{\partial^2 f(x)}{\partial^2 ic\, ia} & \frac{\partial^2 f(x)}{\partial^2 ic\, ib} & \frac{\partial^2 f(x)}{\partial^2 ic} \end{bmatrix} \tag{13}$$

4. Update the trust region radius as in Eq. (14).

$$\Delta_{k+1} = \begin{cases} \tau_3 \Delta_k, & if\ r_k \le \tau_1 \\ \Delta_k, & if\ \tau_1 < r_k \le \tau_2 \\ \min\{\tau_4 \Delta_k, \Delta^-\} & if\ r_k > \tau_2, \|\boldsymbol{d_k}\| = \Delta_k \end{cases} \tag{14}$$

Where $r_k = \frac{f(x_k) - f(x_k + d_k)}{q_k(0) - q_k(d_k)}$

5. Update the solution: If $r_k > \tau_1$ then $x_{k+1} = x_k + d_k$, $B_{k+1} = B_k$, k=k+1 and go to step 1

Else $x_{k+1} = x_k$, k=k+1 and go to step 2

3.2 Levenberg-Marquardt (LM)

The LM optimization method was first introduced in the early 1960's by Levenberg and Marquardt. It combines the gradient descent optimization method with the Gauss-Newton method. Therefore, it is reasonably faster than the gradient method and more stable than the Gauss-Newton method [21]. The LM method behaves like the gradient descent when the current solution is far from optimal and behaves like the Gauss-Newton otherwise [22].

The process of LM method:

1. Set initial guess $\boldsymbol{X_0}, \boldsymbol{\mathcal{J}_0}$ where $\boldsymbol{\mathcal{J}}$ is the damping factor, no.of iteration
2. Compute the cost function $f(\boldsymbol{X_0})$
3. Calculate the Jacobian matrix $\boldsymbol{J}$ and the Hessian $\boldsymbol{H}$
4. Compute $H_{damped} = \boldsymbol{\mathcal{J}} + \boldsymbol{diagonal}\,(\boldsymbol{H})$
5. Calculate the gradient of the cost function $(\nabla f(\boldsymbol{X_0}))$

6. Solve $H_{damped}\, dX = -(\nabla f(\boldsymbol{X_0})$ for dX, which represents the updated direction
7. Update parameters $\boldsymbol{X_{new}} = \boldsymbol{X_0} + \boldsymbol{dX}$
8. Calculate the new cost function $f(\boldsymbol{X_{new}})$
9. Check if $f(\boldsymbol{X_{new}}) < f(\boldsymbol{X_0})$

   Then update $\boldsymbol{\mathcal{J}} = \boldsymbol{\mathcal{J}/10}$ and calculate $f_{diff} = |f(\boldsymbol{X_{new}}) - f(\boldsymbol{X_0})|$

   Else $\boldsymbol{\mathcal{J}} = \boldsymbol{\mathcal{J}} * \boldsymbol{10}$
10. Termination condition

    If $f_{diff} > 10\text{^} - 3$, or no.of iteration <100, then go to step 2

    Otherwise, end

3.3 Application Steps for the Suggested BRB Technique

To implement the proposed BRB detection technique, illustrated in Fig. 1, the following steps are followed:

Step1: Acquire the three-phase stator current signals of a three-phase induction motor. In this work, these currents are obtained from the faulty BRB model.

Step2: Set initial values for the basic parameters (vector $\boldsymbol{X}$ in Eq. (10)) of the motor's mathematical model. The initial values are provided in Table 1, and for practical scenarios, these parameters can be initialized as indicated in [23].

Step3: Calculate the cost function, which is given in Eq. (10).

Step4: Apply the optimization method (TRM or LM) with settings similar to the lsqnonlin solver in Matlab R2023a.

Step5: Obtain the estimated values of the basic parameters that represent the solution of the optimization function.

Step6: Use the trajectory of the estimated rotor resistance to detect the BRB fault

4 Simulation Results and Discussion

The fault detection method is verified in Matlab/Simulink environment R2023a. Table 1 shows the parameters of the used asynchronous motor [13]. The faulty model was run at different numbers of broken rotor bars, and the results of phase 'a' stator current, which are depicted in Fig. 2, are typically the same as those given in [13]. This figure shows that the broken rotor fault generates an envelope in the stator current signals, which is confirmed in [5]. In the same manner, the impact of

the fault on the electromagnetic torque and the speed is shown in Fig. 3. The amount of ripple in the speed and torque signals significantly rises with regard to the fault's severity.

Table 1
Asynchronous motor parameter

Parameter	**Value**
Rated Power	3 hp
Rated Voltage	230 V
Rated Current	9 A
Rotor Resistance	0.816 Ω
Stator Resistance	0.435 Ω
Mutual Inductance	0.0695 H
Stator Inductance	0.0024 H
Rotor Inductance	0.0024 H
Moment of Inertia	0.089 kg.m^2
Load Torque	15 Nm
Number of Rotor Bars	28

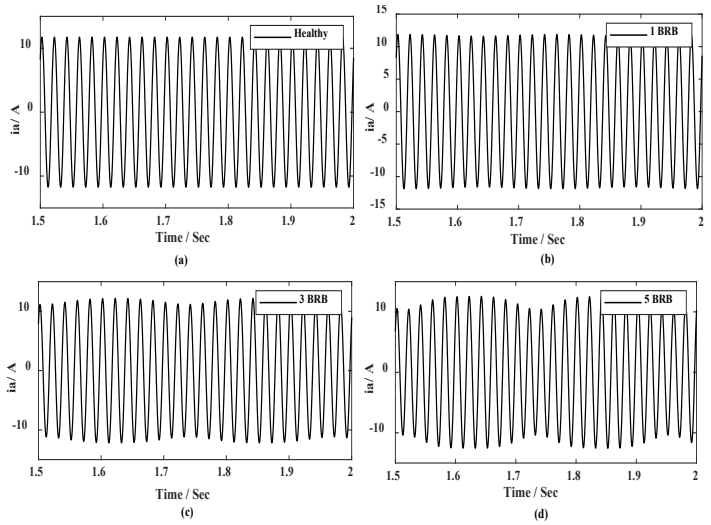

Figure 2
Stator current for (a) healthy condition, (b) one broken rotor bar, (c) three broken rotor bars, and (d) five broken rotor bars

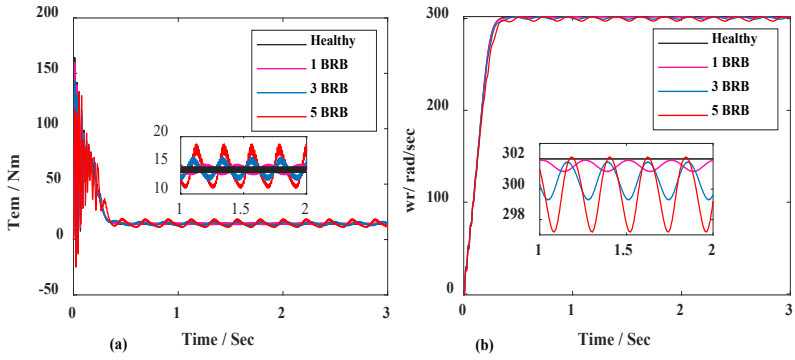

Figure 3

Simulation outcomes for (a) Torque and (b) Speed for healthy, one broken rotor bar, three broken rotor bars, and five broken rotor bars conditions

Fig. 4 and Fig. 5 display the estimated parameters, which are the stator and rotor resistances and inductances, mutual inductance, and load level, obtained by using TRM and L-M optimization methods at healthy and faulty states. While all the parameters change with respect to the load's variation and the broken rotor fault's severity, the rotor resistance shows a distinguishable linear increment with a rapid rise of fault's severity. The behavior of rotor resistance is anticipated as the broken rotor fault leads to an unbalanced rotor magnetic field that results in nonlinear current flow ending up with a higher rotor resistance value. Refereeing to a previous study [24], the rotor resistance and the mutual inductance are the dominant parameters of asynchronous machines. As a result of this, the presence of broken rotor bars can be established via the deviation of the rotor resistance parameter. Table 2 articulates the estimated deviation of the rotor resistance and the mutual inductance from their primary given values under faulty broken rotor bars conditions. Compared to the rotor resistance, the mutual inductance variation is mundane, especially in the case of minor fault intensity (1 BRB).

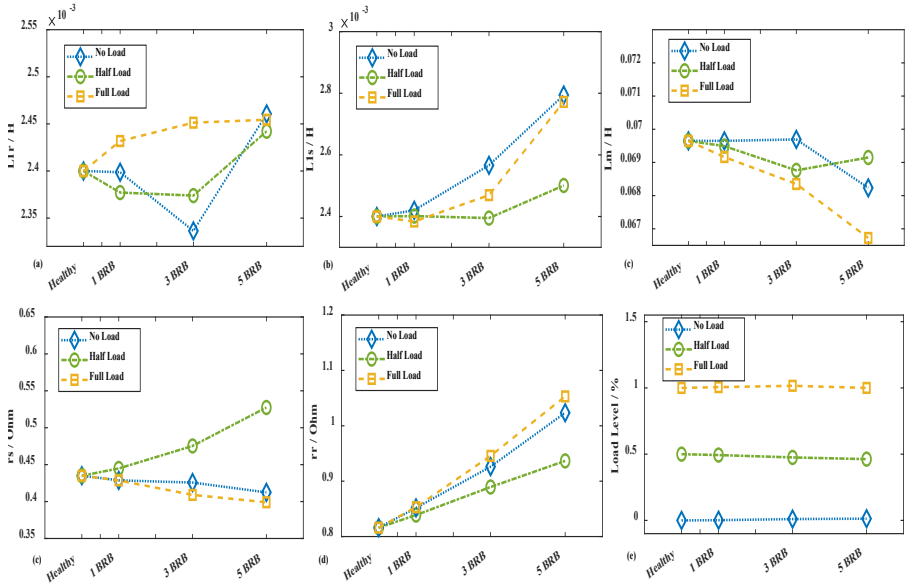

Figure 4

Estimated (a) stator leakage inductance, (b) rotor leakage inductance, (c) mutual inductance, (d) stator resistance, (d) rotor resistance, and (e) load level by TRM at healthy 1 BRB, 3 BRB, and 5 BRB states and at various load conditions.

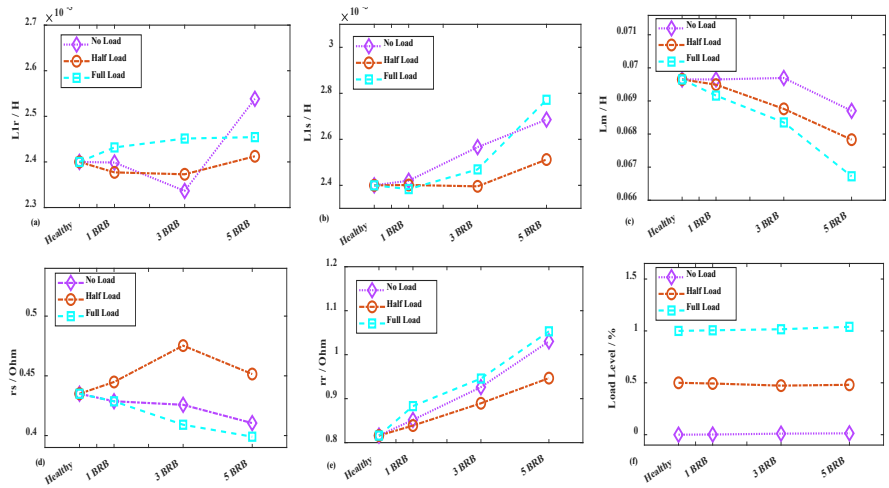

Figure 5

Estimated (a) stator leakage inductance, (b) rotor leakage inductance, (c) mutual inductance, (d) stator resistance, (d) rotor resistance, and (e) load level by L-M at healthy, 1 BRB, 3 BRB, and 5 BRB states and at various load conditions.

Table 2
Deviation of rotor resistance and mutual inductance from the original value at faulty broken rotor bar states

State		Estimated r_r / Ohm	Estimated L_m / H	r_r Deviation / %	L_m Deviation / %
One Broken Rotor Bar	No Load	0.85307	0.069163	4.54	-0.699
	Half Load	0.83881	0.069492	2.79	-0.226
	Full Load	0.85175	0.069651	4.38	0.0001
Three Broken Rotor Bars	No Load	0.94571	0.068351	15.89	-1.865
	Half Load	0.88946	0.068761	9.00	-1.276
	Full Load	0.92624	0.069694	13.51	0.06317
Five Broken Rotor Bars	No Load	1.0531	0.066724	29.05	-4.20
	Half Load	0.93661	0.06783	14.78	-2.613
	Full Load	1.0236	0.068701	25.44	-1.362

The convergence of the TRM and LM for the state of one broken rotor bar fault at no-load, half-load, and full-load is revealed in Table 3. The time consumed to complete the estimation process is also demonstrated in Table 3. This table conveys the optimization methods' success in average estimation time equals 5.3 minutes.

Table 3
Comparison between TRM and LM

State		Starting Cost function value	Cost function minimization by TRM	Cost function minimization by LM	Estimation time consumed by TRM / Minute	Estimation time consumed by LM / Minute
One Broken Rotor Bar	No Load	1036.5	3.5219	3.5219	7	8
	Half Load	302.7676	3.8485	3.8485	4.4	5
	Full Load	10.2689	4.7956	4.7956	4.5	3

To summarize the results, it is recommended that the broken rotor fault be detected by the trajectory of the rotor resistance parameter for the following reasons. Firstly, the parameter linearly rises with the fault's intensity; therefore, fault diagnosis is

possible as well. Secondly, this method is robust against false alarms by other types of faults like an inter-turn fault because it has been proved in [20] that the rotor resistance significantly decreases when the latter fault happens. Finally, estimating the rotor and mutual inductance is mandatory for a machine fed by a drive, making it a cost-effective method. A concise comparison between the proposed approach and recent related works is provided in Table 4.

Table 4
Comparison of this work with recent relevant studies

Reference	BRB Detection Method	Validation against load variation	Robustness against other kinds of fault	Required time for detection	Identifying fault's severity
[5]	Current Envelope and ANN	X	Not verified	Not reported	Yes
[10]	Model-based Kalman filter	X	Not verified	Not reported	Yes
[6]	Model-based SVM	X	Not verified	Not reported	No
[3]	Park's vector product	✓	Robust against inter-turn fault	Not reported	No
This paper	Model-based TRM and LM	✓	Robust against inter-turn fault	5.3 minutes	Yes

Conclusions

Detecting minor broken rotor bar faults in asynchronous motors is an important subject, because this kind of fault, directly threatens the motors' lifespan. A strategic technique based on parameter estimation of a reciprocal healthy asynchronous motor, has been proposed in this study. Two nonlinear optimization methods perform the estimation. Based on the simulation results, the rotor resistance verifies the superior variation, which is linearly increased with the fault's intensity.

From a mathematical viewpoint, this is due to the high impact of the rotor resistance on the model's behavior [24]. Therefore, this paper recommends estimating the rotor resistance parameter, of an asynchronous motor, to detect broken rotor bar faults.

References

[1] G. Niu, X. Dong, and Y. Chen, "Motor Fault Diagnostics Based on Current Signatures: A Review," 2023, *Institute of Electrical and Electronics Engineers Inc.* doi: 10.1109/TIM.2023.3285999

[2] N. A. Dobroskok *et al.*, "Neural network based detecting induction motor defects supplied by unbalanced grid," *International Journal of Power Electronics and Drive Systems*, Vol. 14, No. 1, pp. 185-198, Mar. 2023, doi: 10.11591/ijpeds.v14.i1.pp185-198

[3] A. Allal and B. Chetate, "A new and best approach for early detection of rotor and stator faults in induction motors coupled to variable loads," *Frontiers in Energy*, Vol. 10, No. 2, pp. 176-191, Jun. 2016, doi: 10.1007/s11708-015-0386-2

[4] S. Halder, S. Bhat, and B. Dora, "Start-up transient analysis using CWT and ridges for broken rotor bar fault diagnosis," *Electrical Engineering*, Vol. 105, No. 1, pp. 221-232, Feb. 2023, doi: 10.1007/s00202-022-01657-7

[5] M. O. Mustafa, "Broken Rotor Bars Fault Detection In Induction Motors Based On Current Envelope And Neural Network," *Eastern-European Journal of Enterprise Technologies*, Vol. 3, No. 2-111, pp. 88–95, 2021, doi: 10.15587/1729-4061.2021.227315

[6] M. O. Mustafa, D. Varagnolo, G. Nikolakopoulos, and T. Gustafsson, "Detecting broken rotor bars in induction motors with model-based support vector classifiers," *Control Eng Pract*, Vol. 52, pp. 15-23, Jul. 2016, doi: 10.1016/j.conengprac.2016.03.019

[7] S. Bachir, S. Tnani, J. C. Trigeassou, and G. Champenois, "Diagnosis by parameter estimation of stator and rotor faults occurring in induction machines," *IEEE Transactions on Industrial Electronics*, Vol. 53, No. 3, pp. 963-973, Jun. 2006, doi: 10.1109/TIE.2006.874258

[8] B. Kouadri and A. Hamoudi, "Off-Line Rotor Faults Diagnosis in Induction Machines by Parameter Estimation," 2021 [Online] Available: https://www.researchgate.net/publication/354293953

[9] Rayyam, M., Zazi, M., & Hajji, Y. (2015, November). Detection of broken bars in induction motor using the Extended Kalman Filter (EKF) In *2015 Third world conference on complex systems (WCCS)* (pp. 1-5) IEEE

[10] T. Ameid, A. Menacer, H. Talhaoui, and I. Harzelli, "Rotor resistance estimation using Extended Kalman filter and spectral analysis for rotor bar fault diagnosis of sensorless vector control induction motor," *Measurement (Lond)*, Vol. 111, pp. 243-259, Dec. 2017, doi: 10.1016/j.measurement.2017.07.039

[11] Santos, P. M., Correa, M. B. R., Jacobina, C. B., Da Silva, E. R. C., Lima, A. M. N., Didiery, G., ... & Lubiny. A simplified induction machine model to study rotor broken bar effects and for detection. In *2006 37th IEEE Power Electronics Specialists Conference* (pp. 1-7)

[12] S. Chen and R. Živanović, “Modelling and simulation of stator and rotor fault conditions in induction machines for testing fault diagnostic techniques,” *European Transactions on Electrical Power*, Vol. 20, No. 5, pp. 611-629, Jul. 2010, doi: 10.1002/etep.342

[13] R. Rahmatullah, N. F. O. Serteller, and V. Topuz, “Modeling and Simulation of Faulty Induction Motor in DQ Reference Frame Using MATLAB/SIMULINK with MATLAB/GUIDE for Educational Purpose,” *International Journal of Education and Information Technologies*, Vol. 17, pp. 7-20, Mar. 2023, doi: 10.46300/9109.2023.17.2

[14] R. -E. Precup, E. -L. Hedrea, R. -C. Roman, E. M. Petriu, A. -I. Szedlak-Stinean and C. -A. Bojan-Dragos, "Experiment-Based Approach to Teach Optimization Techniques," in *IEEE Transactions on Education*, Vol. 64, No. 2, pp. 88-94, May 2021, doi: 10.1109/TE.2020.3008878

[15] Kilic, U., Essiz, E. S., & Keles, M. K. (2023) Binary anarchic society optimization for feature selection. *Romanian Journal of Information Science and Technology*, *26*(3-4), 351-364

[16] Precup, R. E., Preitl, S., & Korondi, P. (2007) Fuzzy controllers with maximum sensitivity for servosystems. *IEEE Transactions on Industrial Electronics*, *54*(3), 1298-1310

[17] Zamfirache, I. A., Precup, R. E., & Petriu, E. M. (2023) Q-learning, policy iteration and actor-critic reinforcement learning combined with metaheuristic algorithms in servo system control. *Facta Universitatis, Series: Mechanical Engineering*, *21*(4), 615-630

[18] Ibrahim, S. K., Rad, M. M., & Fischer, S. (2023) Optimal Elasto-Plastic Analysis of Reinforced Concrete Structures under Residual Plastic Deformation Limitations. *Acta Polytechnica Hungarica*, *20*(1)

[19] J. Blanchet, C. Cartis, M. Menickelly, and K. Scheinberg, “Convergence Rate Analysis of a Stochastic Trust-Region Method via Supermartingales,” *INFORMS Journal on Optimization*, Vol. 1, No. 2, pp. 92-119, Apr. 2019, doi: 10.1287/ijoo.2019.0016

[20] R. A. K. Aswad and B. M. H. Jassim, “Impact of Induction Motor Faults on the Basic Parameters’ Values,” *Journal of Engineering*, Vol. 26, No. 12, pp. 66-80, Dec. 2020, doi: 10.31026/j.eng.2020.12.04

[21] Gavin, H. P., “The Levenberg-Marquardt algorithm for nonlinear least squares curve-fitting problems”. *Department of Civil and Environmental Engineering Duke University August*, *3, 2019*

[22] M. Lourakis and M. I. A Lourakis, “A Brief Description of the Levenberg-Marquardt Algorithm Implemened by levmar,” 2005 [Online] Available: http://www.ics.forth.gr/~lourakis/levmar

[23] R. A. K. Aswad and L. Szamel, "Parameter Estimation of Asynchronous Motors Via Trust Region and Pattern Search Optimization Methods," *2023 IEEE 6th International Conference and Workshop Óbuda on Electrical and Power Engineering (CANDO-EPE)*, Budapest, Hungary, 2023, pp. 000119-000124, doi: 10.1109/CANDO-EPE60507.2023.10418029

[24] R. A. K. Aswad and B. M. H. Jassim, "Matlab sensitivity analysis toolbox: an application on faults identification in induction motors," *COMPEL - The International Journal for Computation and Mathematics in Electrical and Electronic Engineering*, Vol. 42, No. 6, pp. 1733-1743, Nov. 2023, doi: 10.1108/COMPEL-12-2022-0445